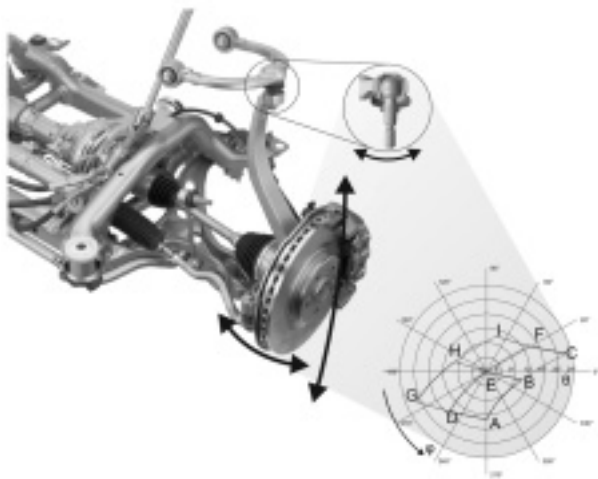


Berechnung und Darstellung von Gelenkwinkeln im Fahrwerk

Calculation and Depiction of Joint Angles in Suspension Systems



Ever shorter times to market and the increasing requirements being made on the functionality of chassis systems necessitate an efficient development process. Careful, advanced development ensures that parameters are integrated at an early stage and conditions for subsequent development can be rapidly and reliably postulated. Together with „ZF Lemförder Fahrwerktechnik“, the „Institut für Kraftfahrwesen Aachen (ika)“ has created a calculation program for use in advanced suspension development.

1 Introduction

The calculation tool ABE has been developed for the purpose of advanced kinematic design for axle systems. This tool is modular and has been continuously further developed. ABE is a tried-and-tested, autonomous development tool, which enables rapid kinematic analysis and advanced design of axles.

ABE has now been extended by a module for calculating the joint angles of ball joints and bushings in the case of axle system rigid kinematic movements. The new joint angle module is capable of evaluating and visualizing the relative joint positions during the movement sequences which occur in an axle system with the two degrees of freedom „spring movement“ and „steering movement“.

2 The Basic Tool ABE

The ABE software tool has been designed for kinematic analysis, for comparing and benchmarking and for rapid, advanced design of axle systems. After inputting the axle's kinematically relevant pivot points (hard points), all characteristic kinematic chassis values are calculated and depicted rapidly. Fast axle system parameter variations and benchmark analyses are possible. Calculation of spatial suspensions (e.g. Multilink) has been enabled. ABE has been implemented in Visual Basic for Applications (VBA) under Microsoft Excel, and can be used license free on virtually any PC. The fast establishment of an axle system and intuitive operation, in particular, make acquisition of the program interest-

Authors:

Ingo Albers and Christoph Elbers

ing, even on-site at the customer's premises, **Figure 1**.

The calculation algorithm is based on a mathematical approach by Matschinsky [1, 2]. This has been implemented in [3] and considerably extended. This approach is used to calculate the translatory and rotational velocity status of the knuckle. The positions and velocities of all involved points within the wheel suspension such as, e.g. the tire contact patch or wheel centre, are therefore explicitly available and are used to calculate the characteristic kinematic values [1, 2, 3], **Table**.

A general five-link mechanism forms the basis of the calculations in ABE, enabling a multitude of different wheel suspension systems to be described (double-wishbone, multilink suspension, etc.). Further suspension types such as, e.g. McPherson suspensions can also be calculated with ABE with the aid of geometrical and kinematic formulations. Describing the steering axis geometry, even in the case of virtual steering axes, in the case of both jounce and steering movements, necessitates extended methods, which are described in full in [3].

3 Joint Movement

When a wheel suspension is moved, control arm movements occur; these are captured as 2-point control arms in ABE. These result in movements in the joints, with which the control arms are fastened either to the vehicle body or the knuckle. In this article, one of the conventional cases in which the control arm is fixed to the body with a bushing and with a ball joint to the knuckle is analyzed as an example. Of course, other configurations are also conceivable.

Different ball joints and bushings are required for each wheel suspension. Besides load dependence, which is not the intended topic of this article, the design is particularly dependent on the kinematic requirements made on the joint. An axle supplier such as ZF Lemförder supplies internally manufactured joints and bushings, and is therefore able to generate conclusions which are vital to internal component development during axle design and advanced development. For example, the maximum angle ranges which are achieved and the joint positions reached over a defined movement cycle are relevant to a ball joint. This information significantly influences the design. In a ball joint, movement between the ball pin and joint housing is kinematically relevant, whilst movement between the inner and outer sleeve is of interest in the case of a bushing, **Figure 2**.

4 Joint Angle Depiction

The relative joint movements are output for visualization in the form of either polar coordinates or a projected 2-plane joint angle depiction. The absolute opening angle can be directly recorded in the polar coordinate depiction. At the same time, the position angle is used to specify the rotational position at which the relevant joint aperture results. In the 2-plane depiction, the position of the deflected joint is described in relation to the initial position via two projection angles. The majority of joint angle depiction methods usual within the industry are thereby covered. **Figure 3**.

Joint rotation around the main joint axis (self-rotation) is also calculated. In the case of a ball joint, self-rotation has an influence

on the joint wear. In the case of a bushing, specification of this joint angle may additionally be used to calculate alignment behaviour and aligning torque, taking material behaviour into consideration.

Whether in polar coordinates or 2-plane projection, the relevant joint position can be clearly read off for each suspension system or knuckle movement status.

5 Wheel Suspension Movement Sequence

A standardized movement sequence has been implemented to guarantee clear assignment of the joint angle results to the relevant movement status and result comparability. After the user has input the maximum jounce travel and maximum tie rod deflection, a movement plan is generated. This plan successively approaches all maximum positions starting from the design position. The spring can jounce and rebound to the maximum positions and the tie rod can be moved to its maximum right-hand and left-hand positions. Together with the initial position, the design position, this results in 9 different terminal positions. In turn, this gives a total of 12 movement paths along which travel occurs, **Figure 4**.

This method therefore efficiently records all extreme kinematic joint statuses, which may arise throughout the wheel suspension's entire movement range. The necessary kinematic angle ranges of the individual joints can therefore be pre-dimensioned during advanced development. The colors of the relevant movement directions and the designations of the relevant key positions in the movement plan are also implemented in the result visualizations to facilitate orientation, see Chapter 11.

6 Fundamental Prerequisites of the Necessary Calculation Operations

In order to calculate the above mentioned joint angles in polar coordinates, in cardanic 2-plane projections and self-rotation, a body-fixed coordinate system has to be defined for each of the two joint components, which are moved in relation to each other. During wheel suspension movement, these coordinate systems move relative to each other. However, only the relevant, local rotations, not the translatory movements, are of kinematic relevance.

If two coordinate systems with the same origin in the inertial system are known, the relative movement of both systems can be determined by depicting the deflected coor-

Table: Excerpt from the list of characteristic kinematic values calculated in ABE

Travel of spring [mm]	Castor angle [°]
Travel of wheel [mm]	Mechanic trail [mm]
Toe angle [°]	Castor offset [mm]
Rack travel [mm]	Spread angle [°]
Steering angle [°]	Scrub [mm]
Camber [°]	Scrub offset [mm]
Tread width [mm]	Disturbing force lever arm (braking) [mm]
Roll centre position (equal & unequal J&R) [mm]	Disturbing force lever arm (accel.) [mm]
Optimal anti-dive angle [°]	Inner steering angle [°]
Actual anti-dive angle [°]	Outer steering angle [°]
Anti-dive percentage [%]	Average steering angle [°]
Optimal anti-lift angle [°]	Differential steering angle [°]
Actual anti-lift angle [°]	Ackermann angle (outer) [°]
Anti-lift percentage [%]	Ackermann percentage [%]
Oblique suspension angle [°]	Steering wheel angle [°]
Spring ratio (spring travel / wheel travel) [-]	Steering ratio [-]

dinate system in the initial status' coordinate system. It is then possible, for example, to describe z-axis deflection in the target system, corresponding to the absolute deflection of the joint which is to be described.

In this case, the initial position is assigned with the index „1“ and the deflected position with the index „2“.

The rotation matrix \underline{A}^{12} rotates the coordinate system from the initial position „1“ to the target position „2“ and therefore receives the given designation:

$$\underline{KS}_2^{(1)} = \underline{A}^{12} \cdot \underline{KS}_1^{(1)} \quad \text{Eq. (1)}$$

The notation for rotation, mapping and coordinate transformation is taken from [4]. $\underline{KS}_2^{(1)}$ means that the coordinate system with the Index „2“ is depicted in the local, non inertial coordinate system „1“ via coordinate transformation.

If target coordinate system „2“ is to refer to the local coordinate system „1“, the following applies:

$$\underline{KS}_2^{(1)} = \underline{A}^{12} \cdot \underline{KS}_2^{(2)} \quad \text{Eq. (2)}$$

\underline{A}^{12} can therefore be used not only to rotate vectors or coordinate systems in space from an initial position to a target position, but also to transform vectors or matrices in various coordinate systems.

Like all of the rotation matrices used in this algorithm, matrix \underline{A}^{12} is orthonormal (orthogonal and normalized) and is therefore subject to the favourable characteristic that the inverse of the transposed matrix applies:

$$\left(\underline{A}^{12}\right)^{-1} = \left(\underline{A}^{12}\right)^T \quad \text{Eq. (3)}$$

7 Allocation of the Coordinate Systems

In order to be able to calculate the joints' movement, the body-fixed coordinate systems of the joint components must be clearly defined. In the case of the vehicle-mounted bushing, orientation of the main joint axis is clearly defined via the centre point of the joint and by specifying a second point on the main axis. Alternatively, the user can accept a proposed joint orientation for the initial analysis steps. In accordance with convention, the main joint axis is regarded as the z-axis. This z-axis and the direction vector of the 2-point control arm connected to the joint span a plane. The x- and y-axes of the initial system are clearly defined by means of a cross product. Coordinate system \underline{B}_1 (bushing system) is therefore clearly and comfortably defined by inputting one individual point on the main joint axis.

The same procedure applies to the ball joint: in addition to the centre point of the joint, the user defines a second point on the ball pin axis (z-axis). Together with the z-axis, the 2-point control arm vector defines the joint's basic plane, and the individual axes of the coordinate system are clearly determined, **Figure 5**. \underline{K}_1 (ball joint system) is therefore also determined.

8 Description of Relevant Body Rotations

As described, the wheel suspension undergoes a prespecified movement plan. In each step, joint deflection is calculated and depicted in relation to the initial status. The initial coordinate systems are defined. The coordinates of the hard points are available from the basic algorithm in ABE. As the ball pin is bolted firmly to the knuckle, these coordinates are also explicitly known.

The relevant 2-point control arm vector which is analyzed is familiar in both its initial and target position from the ABE algorithm. The ball joint housing and the outer bushing sleeve are bound firmly to the control arm and therefore undergo the control arm's full rotation.

The case portrayed here results in the joint movements shown in the **Figure 6** in the event of an even jounce movement.

The Figure shows a control arm, which is rotated upwards out of its design position (black) and into its current target position (white) due to a jounce movement of the wheel. In this figure, only an even rotation is shown. The joint will undergo superimposed spatial rotations in general, which are completely calculated in this algorithm and which are designated as cardanic joint movements. The inertial system is assigned with (0), the system (1) describes the joints' initial position. The target systems are assigned with (2) and (3).

It can also be seen that the ball joint shown here undergoes several movements. Initially, the joint housing rotates along with the overall rotation experienced by the 2-point control arm. Without relative joint movement, the ball joint would assume the light grey position (\underline{K}_2). However, as the ball pin is bolted in the knuckle, it is moved to a new target position (dark grey, \underline{K}_3), with the result that relative ball joint movement between the two positions \underline{K}_2 and \underline{K}_3 is determined.

Due to this superimposed rotation, the ball joint housing reference system first has to be depicted in the corresponding position \underline{K}_2 with the overall rotation matrix:

$$\underline{K}_2^{(1)} = \underline{D}^{12} \cdot \underline{K}_1^{(1)} \quad \text{Eq. (4)}$$

System \underline{K}_3 describes the deflected ball pin, and is determined by the basic ABE algorithm. Like \underline{K}_2 , \underline{K}_3 is known following overall rotation, and is now transformed into $\underline{K}_3^{(2)}$, in order to determine the relevant joint movement relative to \underline{K}_2 :

$$\underline{K}_3^{(2)} = \left(\underline{K}_2^{(0)}\right)^{-1} \cdot \underline{K}_3^{(0)} = \left(\underline{K}_2^{(0)}\right)^T \cdot \underline{K}_3^{(0)} \quad \text{Eq. (5)}$$

The bushing-fixed coordinate system \underline{B}_2 must be depicted as $\underline{B}_2^{(1)}$:

$$\underline{B}_2^{(1)} = \left(\underline{B}_1^{(0)}\right)^{-1} \cdot \underline{B}_2^{(0)} = \left(\underline{B}_1^{(0)}\right)^T \cdot \underline{B}_2^{(0)} \quad \text{Eq. (6)}$$

It can be seen that all matrices, with the exception of transformation matrix \underline{D}^{12} , are known for the relevant control arm which is analyzed.

9 Control Arm Movement and Rotation

Various control arm and joint layouts are possible. Two different versions of the configuration shown here with a bushing and ball joint are initially conceivable. If two control arms are comprised to form a wishbone, describing movement in the event of spring movement, without steering movement, is a simple matter: the momentary axis of the movement runs thorough the two involved, body-mounted bushings (version 1). Thanks to specification of the hard points, this momentary axis is known directly in the global coordinate system. As the wishbone ideally prohibits self-rotation on the part of the two involved struts, overall rotation from the initial to the target position is very simple to describe.

If the two control arms do not form a wishbone, the control arms must be analyzed individually. As a result of this, the self-rotation on the part of the control arm is basically possible in addition to the actual movement to the target position (version 2). The rotation significantly influences the joint angles to be calculated. If the control arm is rotated around its own axis, this rotation can be read off directly as the projection angle α_{yz} or the opening angle ϑ of the relevant joints without any further, superimposed movement.

A rotation matrix which rotates the control arm from its initial position to its deflected position in such a way that the relevant rotation is sensible and realistic therefore has to be found.

As the system analyzed here uses a bushing, a vital characteristic is exploited: the bushing has multi-axial spring characteristics and therefore provides aligning torque in the event of arbitrary deflection. This attempts to move the joint back into its origi-

nal position. In this algorithm, the assumption is therefore made that the control arm's rotation is of precisely the same extent so that, starting from the basic joint position, minimum possible, absolute joint opening takes place.

Control arms and joint configurations other than the one depicted here offer an additional possibility of self-rotation. If the strut is mounted with non-limiting ball joints on both sides, free strut movement around its own axis is possible without any kinematic effects on the overall wheel suspension mechanism (version 3). This is the case in conventional tie rods. In order to nevertheless obtain information on the relative joint angles, the condition that the joining control arm does not reveal rotation around its own axis during overall movement is applied. The resulting joint angles must therefore be regarded as the minimum angles required for the involved joints.

The control arm's initial vector is present as \vec{a}_1 in the calculation algorithm. If the wheel suspension is moved to a position within the movement plan, the control arm's target vector is known as \vec{a}_2 . Rotation matrix \underline{D}^{12} , with which the following applies, is sought:

$$\vec{a}_2^{(1)} = \underline{D}^{12} \cdot \vec{a}_1^{(1)} \quad \text{Eq. (7)}$$

with

$$\vec{a}_1^{(1)} = (\underline{B}_1^{(0)})^{-1} \cdot \vec{a}_1^{(0)} = (\underline{B}_1^{(0)})^T \cdot \vec{a}_1^{(0)} \quad \text{Eq. (8)}$$

and

$$\vec{a}_2^{(1)} = (\underline{B}_1^{(0)})^{-1} \cdot \vec{a}_2^{(0)} = (\underline{B}_1^{(0)})^T \cdot \vec{a}_2^{(0)} \quad \text{Eq. (9)}$$

\underline{B}_1 is known, as is the fact that \vec{a}_2 has the same coordinates in the new coordinate system, \underline{B}_2 , as \vec{a}_1 in \underline{B}_1 :

$$\vec{a}_2^{(2)} = \vec{a}_1^{(1)} \quad \text{Eq. (10)}$$

9.1 Version 1: Wishbone Configuration

For the wishbone with the two known, body-mounted hard points (in this case, P3 and P5), the rotation matrix can be formed directly from the matrices of the control arm-fixed coordinate systems \underline{D}_{D1} in the basic position and \underline{D}_{D2} in the target position:

$$\underline{D}^{12} = \underline{D}_{D2} \cdot \underline{D}_{D1}^{-1} \quad \text{Eq. (11)}$$

$$\underline{D}_{D1} = \left\{ \vec{d}_{1x}, \vec{d}_{1y}, \vec{d}_{1z} \right\} \quad \text{Eq. (12)}$$

With the normalized vector, Eq. (13), the momentary axis of the wishbone is defined by the two body-mounted bushings.

$$\vec{d}_{1z} = \left(\vec{p}_3 - \vec{p}_5 \right)_n = \frac{\vec{p}_3 - \vec{p}_5}{\left| \vec{p}_3 - \vec{p}_5 \right|} \quad \text{Eq. (13)}$$

$\vec{a}_1^{(1)}$ und \vec{d}_{1z} span the bushing's basic plane and \vec{d}_{1y} is located vertically on this:

$$\vec{d}_{1y} = \left(\vec{d}_{1z} \times \vec{a}_1^{(1)} \right)_n \quad \text{Eq. (14)}$$

Finally, \vec{d}_{1x} results directly in Eq. (15), with the result that matrix \underline{D}_{D1} is fully allocated and orthonormal.

$$\vec{d}_{1x} = \vec{d}_{1y} \times \vec{d}_{1z} \quad \text{Eq. (15)}$$

Under the prerequisite that the momentary axis is body-fixed, \underline{D}_{D2} is populated in the same manner and in the same sequence:

$$\begin{aligned} \underline{D}_{D2} &= \left\{ \vec{d}_{2x}, \vec{d}_{2y}, \vec{d}_{2z} \right\} \\ &= \left\{ \vec{d}_{2y} \times \vec{d}_{1z}, \left(\vec{d}_{1z} \times \vec{a}_2^{(1)} \right)_n, \vec{d}_{1z} \right\} \end{aligned} \quad \text{Eq. (16)}$$

The following applies only in the event that the user sets the main joint axes in the involved bushings in the direction of the wishbone's momentary axis \vec{d}_{1z} :

$$\underline{D}_{D1} = \underline{B}_1^{(0)} \quad \text{Eq. (17)}$$

$$\underline{D}_{D2} = \underline{B}_2^{(0)} \quad \text{Eq. (18)}$$

If the main joint axes deviate from this momentary wishbone axis, the bushings are subject to kinematic deflection in the event of wheel suspension movement. This can be consciously applied or avoided.

9.2 Version 2: Free Control Arm Configuration

Calculation of the transformation matrix for version 2 is slightly more extensive. The coordinate system is first described for the bushing in its initial position:

$$\underline{B}_1^{(0)} = \left\{ \vec{b}_{1x}, \vec{b}_{1y}, \vec{b}_{1z} \right\} \quad \text{Eq. (19)}$$

\vec{b}_{1z} is defined via the position of the centre point of the joint and the user's specification regarding the 2nd point on the main joint axis:

$$\vec{b}_{1z} = \left(\vec{p}_{HP} - \vec{p}_{axis} \right)_n \quad \text{Eq. (20)}$$

The control arm vector and the main joint axis also span the joint's basic plane in this case, Eq. (21), with the result that the last remaining unit vector can be calculated:

$$\vec{b}_{1y} = \left(\vec{b}_{1z} \times \vec{a}_1^{(1)} \right)_n \quad \text{Eq. (21)}$$

$$\vec{b}_{1x} = \vec{b}_{1y} \times \vec{b}_{1z} \quad \text{Eq. (22)}$$

In a manner similar to Euler rotation, the subsequent depictational rotation of vector $\vec{a}_1^{(1)}$ to form $\vec{a}_2^{(1)}$ is subdivided into several basic rotations, each around one axis, in order to enable clear and reliable description of the matrices.

To ensure that the bushing undergoes the minimum possible deflection, \vec{a}_1 is first depicted around the z-axis of \underline{B}_1 in an intermediate position „P“. This position has the characteristic that \vec{b}_{1z} and the target vector $\vec{a}_2^{(1)}$ span the xz-plane of the intermediate position.

The first partial rotation (from 1 to P) can therefore be described:

$$\underline{T}_1 = \left\{ \vec{t}_{1x}, \vec{t}_{1y}, \vec{t}_{1z} \right\} \quad \text{Eq. (23)}$$

As rotation is carried out around the z-axis, the following applies:

$$\vec{t}_{1z} = (0 \ 0 \ 1)^T \quad \text{Eq. (24)}$$

Based on the above condition for the xz-plane in P, the following applies, Eq. (25), whereby the last unit vector automatically results as the cross product, Eq. (26).

$$\vec{t}_{1y} = \left(\vec{t}_{1z} \times \vec{a}_2^{(1)} \right)_n \quad \text{Eq. (25)}$$

$$\vec{t}_{1x} = \vec{t}_{1y} \times \vec{t}_{1z} \quad \text{Eq. (26)}$$

This rotational matrix maps $\vec{a}_p^{(1)}$ in the intermediate position:

$$\vec{a}_p^{(1)} = \underline{T}_1 \cdot \vec{a}_1^{(1)} \quad \text{Eq. (27)}$$

With this rotation, the intermediate position vector $\vec{a}_p^{(1)}$ and the target vector $\vec{a}_2^{(1)}$ are now located in a common plane, the xz-plane of system P. The next rotation therefore takes place around the y-axis \vec{p}_y , in order to correctly rotate \vec{a}_p on \vec{a}_2 . To achieve this, both vectors are first transformed into the system P:

$$\vec{a}_2^{(p)} = \underline{T}_1^{-1} \cdot \vec{a}_2^{(1)} \quad \text{Eq. (28)}$$

$$\vec{a}_p^{(p)} = \vec{a}_1^{(1)} \quad \text{Eq. (29)}$$

Direct resolution of this rotation would be possible with the aid of a rotation matrix with trigonometry functions. As, however, such direction cosines are not directionally clear under certain circumstances, the rotational variant with unit vectors is used due to reasons of universal programming.

To accomplish this, \vec{a}_p is first rotated back to a basic axis with \underline{T}_{21} , in order to be subsequently rotated from this basic axis,

with clear unit vectors and \underline{T}_{22} , to the target position:

$$\underline{T}_{21} = \left\{ \begin{matrix} \vec{t}_{21x}, \vec{t}_{21y}, \vec{t}_{21z} \end{matrix} \right\} = \left\{ \vec{a}_p^{(p)}, (0 \ 1 \ 0)^T, \vec{t}_{21x} \times \vec{t}_{21y} \right\} \quad \text{Eq. (30)}$$

$$\underline{T}_{22} = \left\{ \vec{t}_{22x}, \vec{t}_{22y}, \vec{t}_{22z} \right\} = \left\{ \vec{a}_2^{(p)}, (0 \ 1 \ 0)^T, \vec{t}_{22x} \times \vec{t}_{22y} \right\} \quad \text{Eq. (31)}$$

Accordingly, the overall transformation matrix in system P is as follows:

$$\underline{T}_2 = \underline{T}_{22} \cdot \underline{T}_{21}^{-1} = \underline{T}_{22} \cdot \underline{T}_{21}^T \quad \text{Eq. (32)}$$

The initial vector \vec{a}_1 has therefore been rotated step-by-step, taking the control arm's necessary self-rotation into consideration, in vector \vec{a}_2 . The rotation matrix is therefore clearly defined:

$$\vec{a}_2^{(1)} = \underline{D}^{12} \cdot \vec{a}_1^{(1)} = \underline{T}_1 \cdot \underline{T}_2 \cdot \vec{a}_1^{(1)} \quad \text{Eq. (33)}$$

9.3 Version 3: Free, Non-fixed Control Arm Rotation

Control arm self-rotation is prohibited in its entirety in version 3. To achieve this, the transformation matrix is subdivided into basic rotations from the initial status to the target status. As mentioned above, this can be carried out in a manner similar to Euler rotations. In this case, however, rotation with Bryant angles is selected [4]. In contrast, e.g. to the frequently used Euler x convention (z, x, z or 3, 1, 3 rotation) [5], this reveals a rotation sequence which affects all three spatial axes (x, y, z or 1, 2, 3). It is therefore possible to initially rotate the body-fixed coordinate system \underline{B}_1 in such a way that a local, spatial axis is assigned to the control arm vector, in order to then apply such a Bryant rotation. The rotation matrix which rotates around the control arm axis is then set to unit matrix. Therefore, basis rotations takes place only twice without control arm self-rotation.

10 Presentation of Results

If the control arm movement's transformation matrix is known for the individual 2-point control arm, the relative joint movements can be determined, Figure 3.

The following angles can now be read off from the components of the vector which describes the z-axis: the opening angle ϑ the position angle φ and the projected deflection angles α_{yz} and α_{zx} . As the length of the vector is normalized, the two polar angle specifications or the two projection an-

gles are sufficient in each case to fully and completely describe the joint position.

The z-axis is described via:

$$\vec{z} = (z_x \ z_y \ z_z)^T \quad \text{Eq. (34)}$$

This results in the following angle calculations:

Opening angle:

$$\vartheta = \arctan \frac{\sqrt{z_x^2 + z_y^2}}{z_z} \quad \text{Eq. (35)}$$

$$\vartheta = [0, 180^\circ] \quad \text{Eq. (36)}$$

Position angle:

$$\varphi = \arctan \frac{z_y}{z_x} \quad \text{Eq. (37)}$$

$$\varphi = [0, 360^\circ] \quad \text{Eq. (38)}$$

Projection angle in the yz-plane:

$$\alpha_{yz} = \arctan \frac{z_z}{z_y} \quad \text{Eq. (39)}$$

$$\alpha_{yz} = [0, 360^\circ] \quad \text{Eq. (40)}$$

Projection angle in the zx-plane:

$$\alpha_{zx} = \arctan \frac{z_x}{z_z} \quad \text{Eq. (41)}$$

$$\alpha_{zx} = [0, 360^\circ] \quad \text{Eq. (42)}$$

φ , α_{yz} and α_{zx} are defined in sections in this case.

Definition of the angle's origin is important as regards result evaluation and comparability. The rotational direction of the angle specifications follows the mathematically positive directions of the coordinate system.

11 Result Example and Assessment

The result of a joint angle calculation for a knuckle-mounted ball joint in a 5-link suspension is shown as an example in **Figure 7**.

The designations are taken from the movement plan; the four different colours identify the wheel suspension's relevant movement direction. The polar angles ϑ and φ are shown in the left-hand Figure, whilst the two projected joint angles α_{yz} and α_{zx} are shown in the right-hand Figure. These diagrams can be used to inform the component developer of important results, such as e.g. the joint's maximum, absolute deflection (in this case, point C) or the shape of the joint housing orifice A further results diagram regarding the joint's rotation around its own main axis provides other, important information.

Depiction of all of the joint angles which occur throughout a complete movement plan can also provide important data on whether the relevant joint has to be pre-angled in the design position, in order to implement optimized, more efficient joint movement. This results in joint movements with minimized wear or more favourable kinematics.

The approach to calculating and depicting joint angles in the chassis which is described here enables the developer to provide important information for the continued chassis joint development process in an elegant and efficient manner as early as during the advanced development process.

References

- [1] Matschinsky, W.: Radführungen der Straßenfahrzeuge. Berlin, Springer, 1998
- [2] Matschinsky, W.: Bestimmung mechanischer Kenngrößen von Radaufhängungen. Universität Hannover, Dissertation, 1992
- [3] Albers, I.: Erstellung eines Berechnungstools zur starrkinematischen Analyse von Einzelradaufhängungen. Rheinisch-Westfälische Technische Hochschule Aachen, Diplomarbeit, 2003
- [4] Wittenburg, J.: Dynamics of systems of rigid bodies. Stuttgart, Teubner, 1977
- [5] Weisstein, E. W.: Euler Angles. Mathworld, A Wolfram Web Resource, 1999